Catalysis Today 172 (2011) 124–131

Contents lists available at ScienceDirect

Catalysis Today

journal homepage: www.elsevier.com/locate/cattod

The role of Pd–In interactions on the performance of PdIn-Hmordenite in the SCR of NO_x with CH_4

Hernán Decolatti [a], Hanna Solt [b], Ferenc Lónyi [b], József Valyon [b], Eduardo Miró [a], Laura Gutierrez [a,*]

[a] Instituto de Investigaciones en Catálisis y Petroquímica, INCAPE (FIQ, UNL–CONICET), Santiago del Estero 2829, 3000 Santa Fe, Argentina
[b] Institute of Nanochemistry and Catalysis, Chemical Research Center, Hungarian Academy of Sciences, Pusztaszeri u. 59-67, 1025 Budapest, Hungary

ARTICLE INFO

Article history:
Received 25 November 2010
Received in revised form 2 February 2011
Accepted 15 February 2011
Available online 27 March 2011

Keywords:
PdIn-Hmordenite
NO_x-SCR
CO-FTIR
NO adsorption
In–Pd species

ABSTRACT

The aims of this work were to use several techniques to characterize the generated species when indium and palladium were successively exchanged in H-mordenite and to investigate the effect of the Pd/In ratio on the said species as well as to correlate the activity of the prepared solids with the formed moieties. We studied the activity of In-Hmordenite catalysts obtained by reductive solid-state ion exchange and the effect of the addition of Pd. There was a clear correlation between the maximum catalytic activity of each catalyst and its ability to form NO_2 in the temperature-programmed desorption of NO (NO-TPD) experiments performed after NO adsorption. PdInHM(1/3) was the catalyst that showed the best results in activity and, after the first catalytic test, it was further activated. The temperature-programmed reduction (TPR) and NO-TPD results of this solid suggest that the amount of active species increased after the reaction and that there would be some kind of Pd–In interaction. The characterization of the fresh and used samples by CO adsorption and FTIR shows the differences between PdInHM(1/3) and PdInHM(1/6) catalysts in terms of how Pd was present on the support, and justifies the different catalytic behavior of both catalysts.

1. Introduction

In recent years, environmental legislation has become stricter as regards emissions of harmful nitrogen oxides formed by the use of fossil fuels. Small power plants or engines that use natural gas have lower fuel consumption when working under lean conditions, but in this case the abatement of the NO_x emitted is a problem difficult to solve. This is because the traditional methods are not entirely effective. For example, three-way catalysts do not work under lean conditions and the selective catalytic reduction of NO_x with ammonia is not practical due to the corrosivity and toxicity of this gas. In this sense, the proposed reduction of NO_x on zeolitic catalysts or oxides with methane has produced promising results [1,2].

For the reduction of NO_x in exhaust gases, unsaturated hydrocarbons are more reactive than saturated ones [3]. Thus, the development of stable and selective catalysts for the NO_x reduction with methane (CH_4-SCR) in excess of O_2 may be a key improvement applicable to power plants and environmentally friendly vehicles. In this vein, different metals (Pd, Ga, In and Co) exchanged in ZSM5 and ferrierite have been reported as active catalysts for the SCR of NO with CH_4 in the presence of oxygen [4–9]. Concerning the reaction steps, Kikuchi and co-workers [10–12] proposed a bi-functional mechanism for indium and gallium exchanged on H-ZSM-5, by which NO is oxidized to NO_2 in zeolite sites and the NO_2 is reduced to nitrogen by methane at the $(GaO)^+$ or $(InO)^+$ exchanged sites. Thus, it is usually accepted that the oxidation of NO to NO_2 is an important step in the reaction under study [13–15]. Moreover, on In-zeolite catalysts, InO^+ species are associated with a high NO_x adsorption capacity, which in turn favors the reaction rate [16].

Multifunctional catalysts have also been studied, for example Co,Pd-HZSM-5 [17]; Pt,In-HZSM-5 [18]; Ir,In-HZSM-5 [18]; Ce,In-HZSM-5 [19] and PtInFER [20]; showing very promising results. In this vein, we have recently performed an operando DRIFTS study for the PdInHMordenite system, showing that the NO-SCR reaction proceeds through NO^+ and NO_3^- intermediates formed together over the indium oxocations of the In-Hzeolites [21].

Thus, the motivation of this work is to characterize the generated species when both Pd and In are exchanged on the H-mordenite support using the below mentioned techniques, and their impact on the activity for the SCR of NO_x with methane. Since the nature of the active sites is well known, the said reaction is suitable to be used as a test reaction. To this end, Pd and In were exchanged on Hmordenite using different metal proportions.

The samples were characterized by TPR, FTIR of adsorbed CO or NO, TPD of NO, XRD and N_2 adsorption. The catalysts were evaluated for the NO-SCR with methane, and the catalytic properties were correlated with the physical-chemistry characterizations of

* Corresponding author.
E-mail address: lbgutier@fiq.unl.edu.ar (L. Gutierrez).

0920-5861/$ – see front matter © 2011 Elsevier B.V. All rights reserved.
doi:10.1016/j.cattod.2011.02.033

the solids. It is known that the presence of water causes a deleterious effect in catalytic activity when working under real conditions [20]. However, as mentioned above we used the NO_x-SCR as a test reaction, thus we worked without water in the feed.

2. Experimental

2.1. Catalyst preparation

H-mordenite (Süd Chemie AG, Si/Al = 6.7, BET area = 409 m^2/g) and an adequate amount of In_2O_3 (Aldrich; 99.99%) were mixed applying intense co-grinding. By reductive solid-state ion exchange, InH-mordenite (InHM) samples were prepared, reducing the In_2O_3/H-mordenite mixture in H_2 flow at 500 °C for 2 h and then reoxidizing it in O_2 flow at 400 °C for 1 h. The In/Al molar ratios of the obtained mordenite catalysts were 1/6 and 1/3 (3.4 and 6.8 wt%, respectively). Catalysts containing 0.5% Pd (PdInHM and PdHM) were prepared by impregnating the InHM and HM samples with a solution of $Pd(NH_3)_4(NO_3)_2$ and subsequent heating of the samples in O_2 flow at 350 °C for 1 h. Samples with In/Al 1/3 and 1/6 ratios were identified as InHM(1/3) and InHM(1/6), respectively and those containing Pd were called PdHM, PdInHM(1/3) and PdInHM(1/6).

2.2. Catalyst characterization

2.2.1. N_2 adsorption

InHM(1/6), PdInHM(1/6), InHM(1/3) and PdInHM(1/3) catalysts were analyzed by nitrogen adsorption at 77 K using a Micromeritics ASAP 2020 instrument. Prior to the analysis, the solids were degassed under vacuum at 300 °C. To evaluate the sorption isotherms in terms of specific surface area and micropore volume, BET and t-plot analyses were applied. The specific surface area, the external surface area and the micropore volumes derived from the t-plot are standard values for the characterization of porous materials.

2.2.2. Temperature-programmed reduction

An Okhura TP2002S instrument equipped with a TCD detector was used. The samples were pretreated in N_2 flow at 350 °C for 1 h and the reduction was performed with a mixture of 5% H_2/Ar with a temperature ramp of 10 °C/min up to 900 °C. The TCD signal was calibrated using a CuO standard sample in order to accurately quantify the hydrogen consumption during the TPR experiments.

2.2.3. Temperature-programmed desorption of NO (NO-TPD)

It was conducted in a flow equipment with controlled gas flow and heating. The desorbed gases (NO, N_2O and NO_2) were monitored and quantified with a Fourier transformed infrared spectrometer (FTIR), Thermo Mattson Genesis II, equipped with a gas cell with CaF_2 windows. The adsorption of NO was performed at room temperature for 20 min. Then, we made a sweep to remove NO from the gas phase and that reversibly adsorbed. After that, the reactor was heated at 5 °C/min in He flow and a spectrum of desorbed gas phase was taken every 2 min (10 °C).

2.2.4. CO adsorption followed by FTIR analysis

The adsorption was carried out using a glass cell with CaF_2 windows consisting of a body in which a self-supported catalyst pellet could be treated with H_2 and/or evacuated to 1.3×10^{-7} kPa. FTIR spectra were obtained at room temperature with a Shimadzu Prestige 21 instrument. Prior to the reading of the spectrum, the pellets were reduced with H_2 at 400 °C for 1 h and evacuated to 1.3×10^{-7} kPa for 8 h at 400 °C (reduced sample), or subject only to the vacuum treatment (calcined sample). A spectrum was acquired before the adsorption of CO and adopted as a reference for background subtraction at room temperature. Spectra were taken consecutively after the addition of 1.07, 2.14, 5.33 and 12 kPa of CO. All the spectra shown in this work were normalized at the same weight/surface wafer ratio.

Table 1
Catalytic activity of the prepared solid for the NO_x SCR with methane.

Catalysts	NO to N_2 conversion (%)			
	350 °C	400 °C	450 °C	550 °C
InHM(1/3)	29[a]	14	6	7
PdInHM(1/3)	38	41	31	44[a]
PdInHM(1/3) (2nd test)	48	59[a]	31	48
InHM(1/6)	36[a]	21	11	10
PdInHM(1/6)	31[a]	15	5	9
PdInHM(1/6) (2nd test)	28[a]	13	6	8
PdHM	9	23	29	43[a]

Reaction conditions: see Section 2.
[a] Maximum conversion.

2.2.5. NO adsorption followed by FTIR analysis

These experiments were carried out with the same spectrometer used for NO-TPD experiments. Finely powdered catalysts were pressed (6×10^5 kPa, 5 min) into self-supporting wafers. Each wafer was inserted into a quartz sample holder with a furnace for the *in situ* activation of the sample. The sample holder was attached to the IR cell with CaF_2 windows. After the pretreatment program, it was allowed to cool to room temperature and the spectrum of the activated sample was collected. The adsorption procedure involved contacting the activated wafer with NO at RT for 15 min and outgassing with He to remove the NO gas-phase. Then, the temperature was increased in steps (100, 120, 150, 200 and 250 °C) and a FTIR spectrum at RT was collected after each step.

2.2.6. X-ray diffraction study

The X-ray diffraction measurements were taken using an XD-D1 model Shimadzu diffractometer operated with Cu Kα radiation at 30 kV and 40 mA, using a scanning rate of 1° min^{-1}. The database employed was the one provided by the manufacturer.

2.3. Catalytic test

The powder catalysts were evaluated using the same flow reactor described in the NO-TPD experiments. The typical composition of the reagent stream was: 4000 ppm CH_4, 4000 ppm NO and 2% O_2 (GHSV: 15,000 h^{-1}). The reactor effluent composition was monitored for CH_4, CO, NO, N_2O and NO_2 by FTIR. In some of the experiments, a TCD chromatograph was used in order to verify the conversion and selectivity values obtained with the FTIR detector, founding an excellent agreement between the two methods of analysis.

3. Results and discussion

3.1. Catalytic activity

The InHM(1/3) and PdInHM(1/3) catalytic activity values for the selective catalytic reduction of NO to nitrogen are shown in Table 1. It can be observed that the presence of Pd significantly promotes the activity of the catalyst (from 29% to 41%). On the other hand, an activation phenomenon occurs under reaction conditions above 500 °C.

The InHM(1/3) and InHM(1/6) catalysts (Fig. 1A and B, respectively) have a NO to N_2 conversion with the typical shape of a volcano, where the conversion decreases at a certain temperature because of the undesired methane combustion. However, the presence of Pd in PdInHM(1/3) leads to a gradual increase

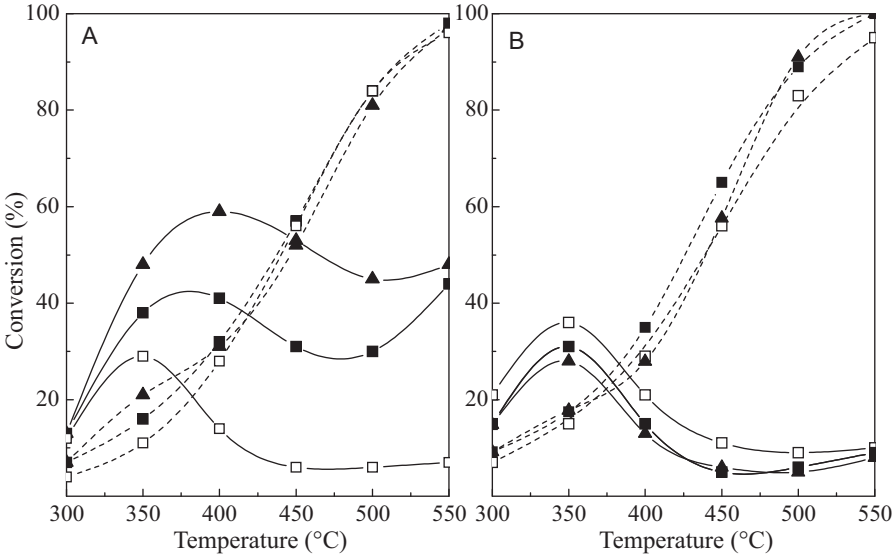

Fig. 1. Catalytic activity of InHM and PdInHM catalysts. Solid lines: NO to N_2 conversion. Dash lines: CH_4 to CO_2 conversion. (A) In/Al = 1/3 (□: InHM(1/3), ■: PdInHM(1/3) initial test, ▲: PdInHM(1/3) second test); (B) In/Al = 1/6 (□: InHM(1/6), ■: PdInHM(1/6) initial test, ▲: PdInHM(1/6) second test). GHSV: 15,000 h^{-1}.

of NO_x conversion at temperatures above 500 °C. This activation phenomenon is permanent and on a second test, the NO to N_2 conversion is greater while the CH_4 to CO_2 conversion does not change significantly in the temperature range studied. This could indicate that during the reaction the species present in the catalyst would suffer certain changes that lead to the increase of active sites for either NO_x adsorption or activation. This behavior suggests that the calcination at 400 °C is not enough to develop the active species. Thus, during the reaction at higher temperatures more active sites are formed which leads to higher activity and selectivity (Fig. 1A). This interesting aspect, which is related to the development of the active species, will be further discussed in the characterization section.

Besides, in the samples with lower content of indium (In/Al = 1/6), it can be observed that the addition of Pd leads to a different behavior (Fig. 1B). The NO to N_2 conversion values are lower than those obtained with InHM(1/6). Furthermore, when we subjected the PdInHM(1/6) catalyst to a second catalytic evaluation, no activation phenomenon was observed as the one recorded in the PdInHM(1/3) catalyst (Fig. 1A). This suggests that the proportion of indium in the catalyst is a predominant factor in the promoting effect of Pd.

We also studied the behavior of the PdHM catalyst and noted that the NO to N_2 conversion reached a maximum NO_x conversion of 40% at 550 °C, (Fig. 2). We observed that the activation process recorded in PdInHM(1/3) does not occur in the monometallic catalysts (PdHM and InHM). Then, it can be concluded that the activation phenomenon must be originated in changes occurred due to Pd–In interactions.

It should be remarked that the formation of N_2O was not detected in the composition of the products evaluated by FTIR (the typical signal of N_2O at 2137 cm^{-1} was absent in all the experiments).

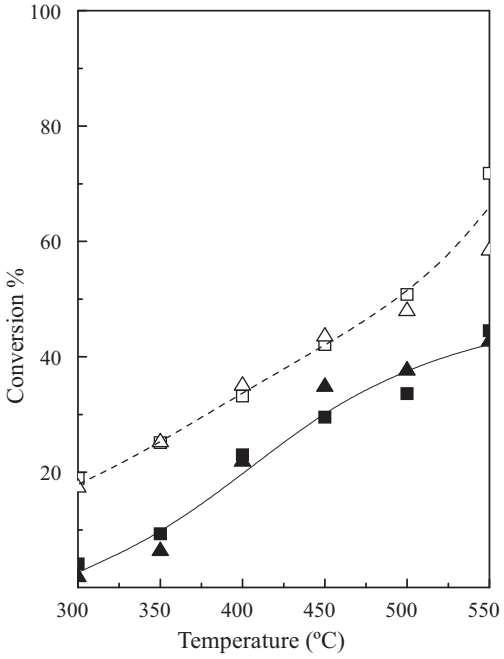

Fig. 2. Catalytic activity of the PdHM catalyst. Solid lines: NO to N_2 conversion (■: initial test, ▲: second test) Dash lines: CH_4 to CO_2. Conversion (□: initial test, △: second test). GHSV: 15,000 h^{-1}.

3.2. Catalyst characterization

3.2.1. Nitrogen adsorption

Table 2 shows a summary of nitrogen adsorption results. The BET surface area of the parent mordenite is 409 m^2/g and decreases with

Table 2
N_2 adsorption results.

	Calcined catalysts			
	InHM(1/6)	PdInHM(1/6)	InHM(1/3)	PdInHM(1/3)
BET surface area: (m^2/g)	355.37	371.52	335.01	339.35
t-Plot micropore area: (m^2/g)	314.19	348.98	292.17	302.17
t-Plot external surface area: (m^2/g)	41.17	22.54	42.84	37.18

BET Surface area of the parent sample (H-mordenite) is 409 m^2/g.

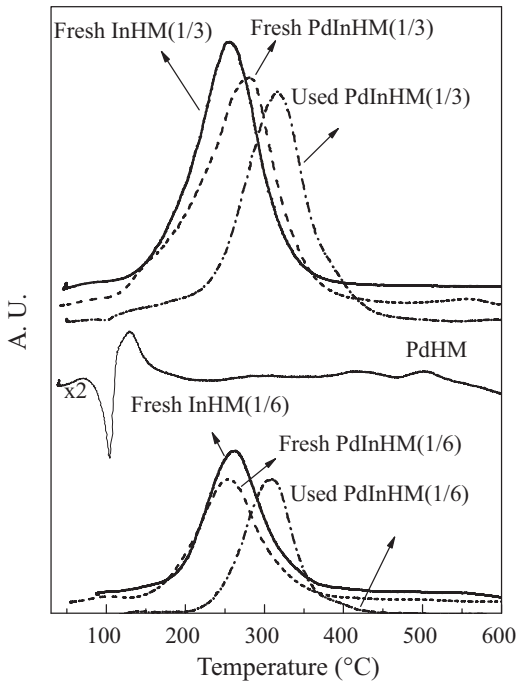

Fig. 3. Temperature-programmed reduction profiles of the PdHM, InHM and PdInHM catalysts. Solid lines: monometallic catalysts, dash lines: bimetallic catalysts.

the indium exchange as a consequence of the presence of bulky InO^+ species inside the mordenite channels. In this way, the sample with the highest In content has the lowest surface area.

3.2.2. Temperature-programmed reduction (H_2-TPR)

The TPR results of the fresh and used catalysts are shown in Fig. 3, whereas Table 3 shows the corresponding H_2 consumption.

3.2.2.1. Fresh catalysts. The TPR of monometallic catalysts was carried out as reference. For the PdHM sample, the negative peak at 106 °C is attributed to some hydrogen produced during the decomposition of the palladium hydride β phase [22], which is formed by dissolution of hydrogen inside the metal particles of palladium at room temperature and under the reducing mixture. The first hydrogen consumption overlaps the negative peak. This low temperature peak could relate to oxidized Pd species at the external surface of the zeolite as these are likely the first ones to be reduced. It is well known that wet impregnation could result in larger PdO clusters deposited at the external surface of mordenite. The peaks between 420 °C and 505 °C could represent reduction of Pd-oxo species and Pd cations in the mordenite pores formed during the calcination of these catalysts or simultaneously during the impregnation process ($PdO + H^+ \rightarrow Pd(OH)^+$). These particles are obviously reduced at higher temperature than PdO, which could explain the peaks observed at higher temperatures in the TPR profile.

For both InHM samples, the main reduction peak is below 400 °C suggesting the presence of $(InO)^+$ at zeolite exchange positions which is associated with active species for the CH_4-SCR of NO_x [23]. No reduction peaks are observed at temperatures higher than 600 °C; therefore, it could be inferred that there is no highly crystalline In_2O_3 in the matrix. The asymmetry and the large width of the thermograms could also be associated with the contribution of some highly dispersed In_xO_y particles. The XRD patterns of the samples (not shown) confirmed the absence of bulk In oxide, which is consistent with the absence of high-temperature peaks in the TPR results. The XRD results also verified that after reaction neither a change in the structure of solids nor segregation of oxides is observed.

The addition of Pd to InHM(1/3) leads to a slight increment (0.88–0.96) in the H_2/In consumption ratio probably due to the reduction of Pd species. Note that H_2/(In + Pd) ratio is 0.89 (Table 3). On the other hand, the maximum reduction temperature (TM) increases by 25 °C (260–285 °C). Such difference may be due to the presence of highly dispersed In_xO_y favored by the palladium particles.

On the contrary, when palladium is present in the InHM(1/6) catalyst the hydrogen consumption decreases (H_2/In = 0.92–0.65) but the maximum temperature almost does not change. It could be suggested that the behavior of the catalysts depends not only on the In/Al ratio but also on the Pd/In ratio that would lead to different interactions between Pd and In species and/or with the solid surface.

Table 3
Temperature-programmed reduction. H_2 consumption on calcined and used catalysts.

Catalysts		H_2 consumption		
		H_2/In[a]	H_2/(Pd + In)[a]	TM (°C)[b]
InHM(1/3)	Fresh	0.88	–	260
	Used	0.80	–	232
PdInHM(1/3)	Fresh	0.96	0.89	285
	Used	0.83	0.77	320
InHM(1/6)	Fresh	0.92	–	260
	Used	0.74	–	238
PdInHM(1/6)	Fresh	0.65	0.56	255
	Used	0.58	0.50	306

[a] Molar ratio.
[b] Peak maximum temperature.

3.2.2.2. Used catalysts. For all the catalysts studied in this work, the amount of hydrogen consumed during the TPR experiments decreased after their use under reaction conditions. This could be due to the presence of some Pd–In interaction that leads to a lower reducibility of indium exchanged species, or to a decrease in the amount of those. However, the trend followed by the temperature for maximum reduction rate is different. For both InHM samples, TM decreases similarly (profiles not shown), whereas for both Pd containing samples the contrary occurs. This opposite behavior indicates that Pd–In interactions actually exist, and that their characteristics changed under reaction conditions. Thus, the different reaction behavior observed when comparing PdInHM(1/3) and PdInHM(1/6) could be related to the amount of reducible species of the used samples. The former, which has a higher activity, shows a H_2/In ratio of 0.83, while for the second the ratio is 0.58. However, this behavior does not explain the activation under reaction conditions observed for PdInHM(1/3). Note that for the fresh sample the H_2/In ratio is 0.96 and after reaction the value is 0.83. Thus, further characterization tools are needed, and they are discussed in the following sections.

3.2.3. Temperature-programmed desorption of NO (NO-TPD)

In order to understand the different effects of the incorporation of metallic palladium in InHM catalysts, NO temperature-programmed desorption experiments (NO-TPD) were carried out. The results are detailed in Table 4 and Figs. 4 and 5. NO_2 desorption besides NO were observed in all solids, at different rates depending on the In/Al, Pd/In ratios and on whether the solids were fresh or used. We performed gas-phase experiments, and it was confirmed that the NO to NO_2 conversion was negligible in the absence of the catalyst and under the experimental conditions of our experimental system.

Table 4
Temperature-programmed desorption of NO_x.

Catalysts		NO-TPD			
		NO/In	NO_2/In	NO_2/(In + Pd)	NO_2/NO
InHM(1/3)	Fresh	0.59 (85 °C)	0.57 (180 °C)	–	1.00
	Used	0.48 (110 °C)	0.67 (180 °C)	–	1.40
PdInHM(1/3)	Fresh	0.61 (100 °C)	1.16 (160 °C)	1.07	1.90
	Used	0.42 (145 °C)	1.35 (160 °C)	1.25	3.20
InHM(1/6)	Fresh	0.55 (120 °C)	1.00 (165 °C)	–	1.82
	Used	0.56 (110 °C)	0.70 (165 °C)	–	1.25
PdInM(1/6)	Fresh	2.54 (110 °C)	1.37 (170 °C)	1.18	0.54
	Used	0.91 (135 °C)	0.32 (190 °C)	0.27	0.35
		NO/Pd	NO_2/Pd	NO_2/(In+Pd)	NO_2/NO
PdHM	Fresh	0.26 (175 °C)	0.68 (230 °C)	–	2.58

The NO_2 formation is associated with the presence of adsorbed oxygen on the zeolite surface [24] or the oxidation of adsorbed NO on In associated species (InO^+ at exchange positions or In_xO_y species). The addition of Pd to InHM(1/3) leads to a very different NO_x desorption with respect to the corresponding monometallic catalysts (Fig. 4A and B). NO_2 desorption peaks increase, and the NO_2/In ratio is higher than one, probably due to the reduction of Pd-oxo species. Another way to explain this behavior is the possibility of the decomposition of NO molecules on Pd sites, giving place to adsorbed oxygen species, which in turn are able to oxidize NO.

Besides, the increase in the amount of NO_2 formed during the NO adsorption on the used PdInHM(1/3) catalyst suggests a greater amount of oxygen species associated with the network or the indium in the matrix. This increase of the active species could explain the increase in NO conversion observed in the reaction conditions.

The NO_x desorption on the fresh InHM(1/6) solid is similar to that on the used one (Fig. 5A). A decrease is observed in the desorbed NO_2/NO ratio. This could indicate that for this In/Al ratio the InO^+ species have more interaction with the structure, which makes them more stable.

Used and fresh PdInHM(1/6) catalysts (Fig. 5B) have a lower NO_2 desorption capacity compared to that of PdInHM(1/3). This suggests the presence of labile oxygen, less exposed to the oxidation of NO. Finally, we can conclude that the promoting effect of Pd on the adsorption capacity is closely related to the In/Pd ratio in the zeolite matrix.

The palladium contribution to the NO_2 formation was supported by performing NO-TPD on PdHM. The NO-TPD results of the PdHM catalyst (Fig. 6) show a high NO_2/NO ratio. This confirms that Pd is involved in the formation of NO_2 in the PdInHM catalysts.

From the catalytic results and solids characterization by NO-TPD, it can be noted that there is clearly a correlation between the maximum catalytic activity obtained for each catalyst and the NO_2 and NO desorbed ratio. Fig. 7 shows that when this ratio increases, the catalytic activity also increases; so, we can say that it is influenced by the catalyst ability to form NO_2. The monometallic Pd catalyst does not fit in this correlation, probably because the reaction mechanism is different. Since we did not measure the amount of NO adsorbed, we cannot rule out the possibility that the higher catalytic activity of Pd promoted catalysts may also be due to a higher adsorption capacity of NO.

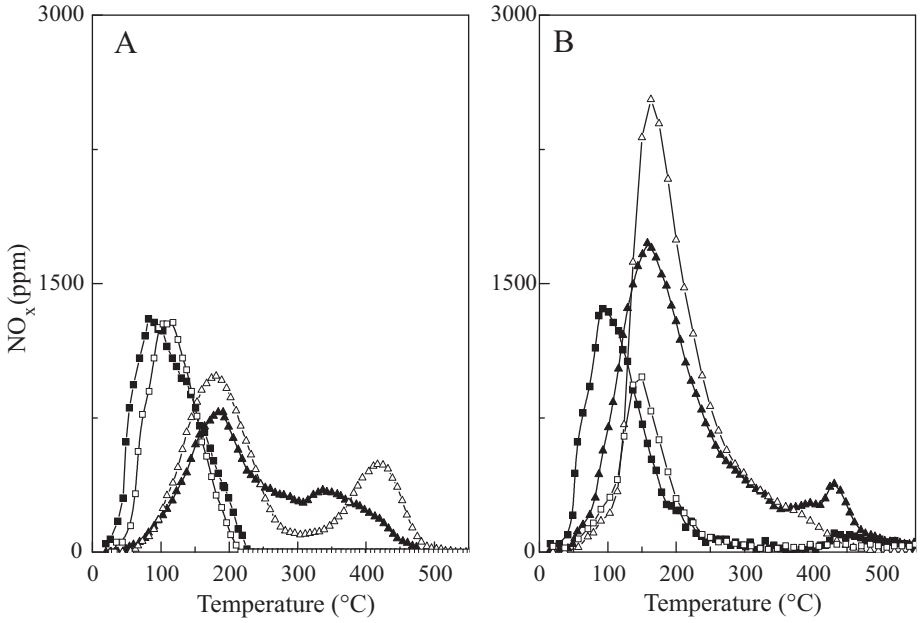

Fig. 4. NO_x-Temperature programmed desorption (NO-TPD). (A) InHM(1/3) catalyst. (B) PdInHM(1/3) catalyst. Filled symbols: fresh catalyst. Empty symbols: used catalyst (■, □: NO desorption; ▲, △: NO_2 desorption).

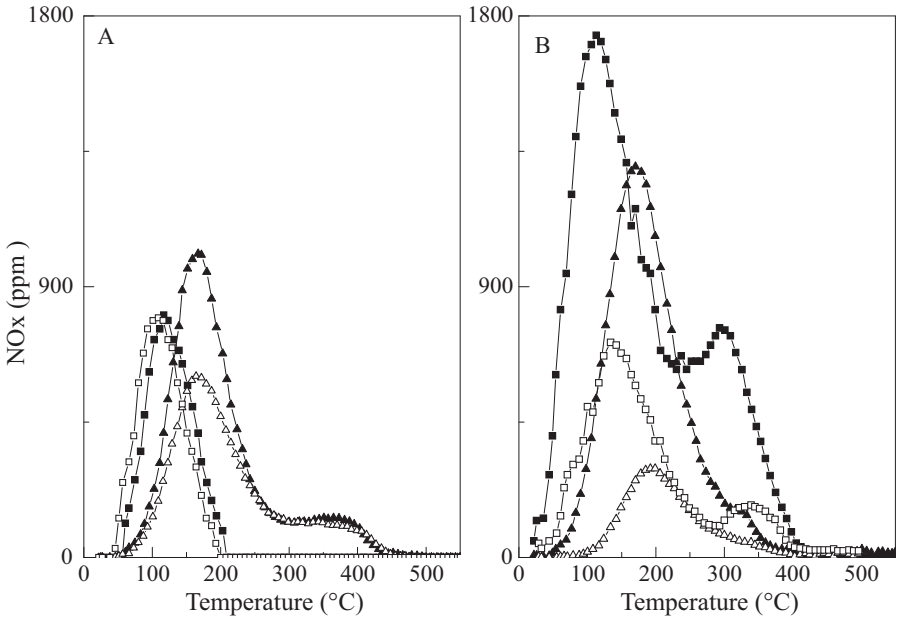

Fig. 5. NO_x-Temperature programmed desorption (NO-TPD). (A) InHM(1/6) catalyst. (B) PdInHM(1/6) catalyst. Filled symbols: fresh catalyst. Empty symbols: used catalyst (■, □: NO desorption; ▲, △: NO_2 desorption).

3.2.4. CO adsorption followed by FTIR analysis

This technique was used in order to obtain more information about the physicochemical characteristics on the surface of solids under study. The CO adsorption spectra observed on the calcined HM support (Fig. 8a) was the typical ones for H-Mordenite reported by several authors [25,26]. Accordingly, in the CO stretching range the band at 2220 cm^{-1} together with that at 2193 cm^{-1} can be assigned to carbon monoxide molecules strongly interacting with extra-framework aluminum species (Lewis acid sites), often observed in de-aluminated zeolite systems and the band that appears at 2168 cm^{-1} is assigned to Brönsted acid sites [5]. By increasing the coverage, a strong IR absorption band develops at about 2140 cm^{-1} due to CO physisorption inside the mordenite channels, a phenomenon arising at higher equilibrium pressures.

Hadjiivanov and Vayssilov [27] summarized data characterizing the adsorption of CO on oxide surfaces and zeolites by IR spectroscopy. They reported that the general spectral ranges which have been attributed to surface Pd^{n+} carbonyls are 2215–2110, 1995–1975, and ~1930 cm^{-1}. Linear complexes Pd^{2+}-CO are characterized by bands between 2215 cm^{-1} and 2145 cm^{-1}. Pd^{+}-CO species were observed at 2140–2110 cm^{-1}.

In the 1995–1975 cm^{-1} range or around 1930 cm^{-1}, the signals were assigned to Pd^{+}-CO-Pd^{+} carbonyl bridge. The complex $Pd^{2+}(CO)_2$ was assigned to 2160–2140 and 2125 cm^{-1} (corresponding symmetric and antisymmetric stretching). $Pd^{3+}(CO)_2$ species

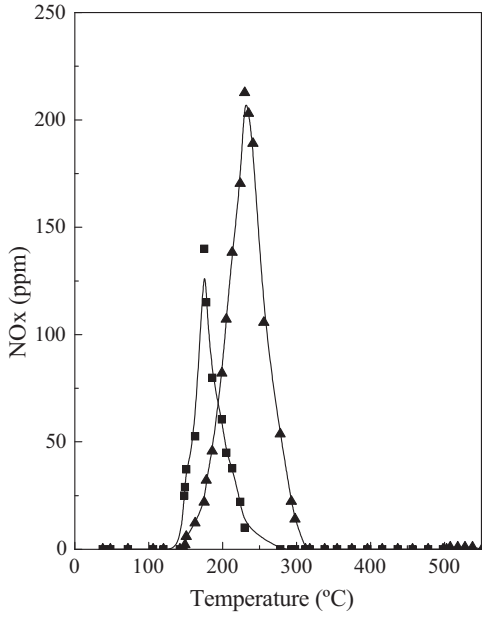

Fig. 6. NO_x-Temperature programmed desorption of the PdHM catalyst (NO-TPD): (■: NO desorption; ▲: NO_2 desorption).

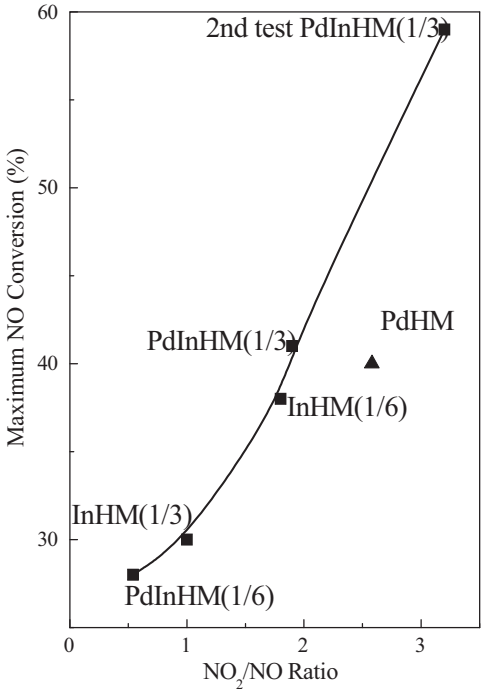

Fig. 7. Desorbed NO_2/NO ratio vs catalytic activity.

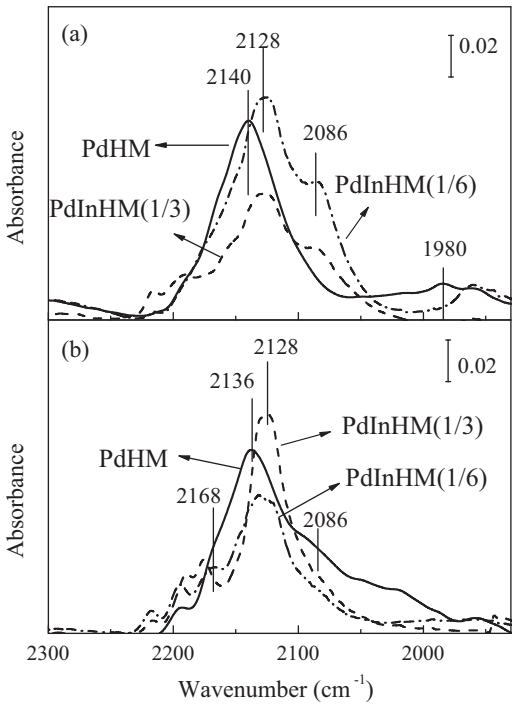

Fig. 8. FTIR spectra of adsorbed CO: (a) calcined solids; (b) reduced solids. P_{CO}: 0.65 kPa.

are also characterized by a pair of bands at 2215 and 2197 cm^{-1} [28]. The CO adsorption bands appearing below 2100 cm^{-1} are generally attributed to carbonyl forms of metallic Pd [29].

Fig. 8a and b show the spectra of adsorbed CO at 5.33 Kpa on HM, PdHM and bimetallic samples.

PdHM: the calcined catalyst with 0.5 wt% palladium has a main asymmetric band of adsorbed CO-FTIR at 2140 cm^{-1} assigned to Pd^{2+} at exchange positions (Fig. 8a). This band has a tail towards lower frequencies due to the contribution of some external Pd^0 species produced during CO exposure. In addition, two shoulders are insinuated in 2167 and 2150 cm^{-1} due to the presence of complexes as $Pd^{2+}(CO)_2$. These results may suggest that palladium is highly dispersed in the matrix. The weak bands around 1980 cm^{-1} are due to CO entities associated as a bridge to Pd^{2+} species. When the wafer is reduced with pure H_2 at 400 °C, after adsorption of CO, the band at 2136 cm^{-1} is the most important one (Fig. 8b).

The small shift to lower frequencies of the main band and the small loss of intensity compared with the main band before reduction (2140 cm^{-1}) suggests that palladium is not completely reduced. A shoulder at 2086 cm^{-1} confirms the presence of metallic palladium.

PdInHM(1/6): Fig. 8a shows that calcined PdInHM(1/6) adsorbs CO and the developed bands are assigned to CO adsorbed on Pd^+ species (2128 cm^{-1}). The presence of a CO-Pd^0 band suggests the reduction of Pd^{2+} due to the presence of CO. There is no evidence of Pd^{+2} species suggesting that there would be no interaction of palladium with the indium or the formation of intermetallic species.

It should be considered that the absence of the CO adsorption band of Pd^{2+} may be due to the partial reduction of PdO to Pd^+ by the presence of CO; this effect depends on the interaction of oxidized Pd particles with their neighbourhood.

When the PdInHM(1/6) catalyst is reduced (Fig. 8b) the main band for CO adsorbed on partially reduced palladium is maintained while the signal of metallic palladium appears as a shoulder at 2086 cm^{-1}. This behavior may be due to the migration of reduced palladium to hidden positions or agglomeration of Pd^0 particles on the surface of the mordenite. This hypothesis can be correlated with the appearance of higher CO pressures of a band of Brönsted sites at internal sites of the zeolite at 2168 cm^{-1} (not shown). The intensity loss of the spectra after the reduction treatment also suggests the migration of palladium particles in the channels of mordenite or some agglomeration. The presence of the Pd^+-CO band, even after the reduction treatment, is also compatible with the presence of any strong Pd–In interaction or with the presence of intermetallic particles.

PdInHM(1/3): the spectra of adsorbed CO obtained on calcined PdInHM(1/3) is shown in Fig. 8a. The broad bands indicate the contribution of several species, including Pd^{2+}, Pd^+ and Pd^0. After reduction, the spectra became narrower and increased their intensity, the main band for CO being adsorbed on Pd^+ species. As noted in PdInHM(1/6), the CO-Pd^0 signal decreased after the reduction, but in this case the probability that the palladium migrates within the structure is lower due to the high ratio of indium. Therefore, it is likely that the palladium, which in the calcined sample presented an adsorption band at 2084 cm^{-1} be associated with the Indium species during the hydrogen reduction process so that the Pd–In interaction increases or new intermetallic species are formed.

We observed that in both used PdInHM catalysts, the CO adsorption capacity decreased significantly and their respective spectra were different (not shown). We noted that the adsorption bands corresponding to the support (HM) were comparable to the used catalysts, which contained Pd and In. This effect could be explained by the migration of species to hidden positions into the matrix, or to a different distribution of the particles that led to a higher interaction between In and Pd. In PdInHM(1/6) the presence of Pd^{2+}, Pd^+ and Pd^0 was observed while in the CO adsorption spectra of PdInHM(1/3), the band associated with Pd^0 was not present. The presence of the signal of Pd^0 on the used PdInHM(1/6) may be due to the labile oxidized palladium that is easily reduced by CO, suggesting a lower interaction of Pd with the matrix and/or with indium than in the used PdInHM(1/3) catalyst.

3.2.5. NO adsorption and FTIR study

NO is a strong Lewis base and when it has a σ-bonded interaction, it is more firmly adsorbed on cationic sites. In order to explain the results obtained with the NO-TPD experiments and to elucidate the Pd–In interaction, the IR spectra of the PdHM and PdInHM(1/3) catalysts after the adsorption of NO were obtained (Fig. 9).

Adsorption of NO on PdHM and PdInHM(1/3) results in the appearance of a series of bands in the 2200–1700 cm^{-1} range. The bands with maxima at 1881 and 1836 cm^{-1} characterize nitrosyl complexes of palladium cations, and they are assigned to Pd^{2+}-NO and Pd^{2+}-(H_2O)(NO), respectively [30]. The presence of the broad bands in the 1600–1700 range may be due to the formation of nitrate/nitrite groups resulting from the reaction of NO_x with the zeolite surface and/or water [31,32] or to NO_2 adspecies [33]. On the other hand, Anunziata and co-workers [34] studied the adsorption of NO on InZSM5 catalysts and reported the presence of two species adsorbed on InO^+ at exchange position, one at 1575 cm^{-1} corresponding to NO_2 and the other at 1622 cm^{-1} which can be assigned to adsorbed (ONO)–. After a close observation of the PdHM catalyst spectra, the last bands were not observed or were negligible.

Note that on the PdHM solid, the Pd^{2+}-NO bands and the signals between 1600 and 1700 cm^{-1} decreased with the increment of temperature, while for PdInHM(1/3) they increased, possibly because the formation of NO_2 and nitrite species was favored by the presence of indium and the increment of temperature. These results may explain the ability of PdInHM(1/3) to produce NO_2 and, consequently, the higher activity of the bimetallic sample.

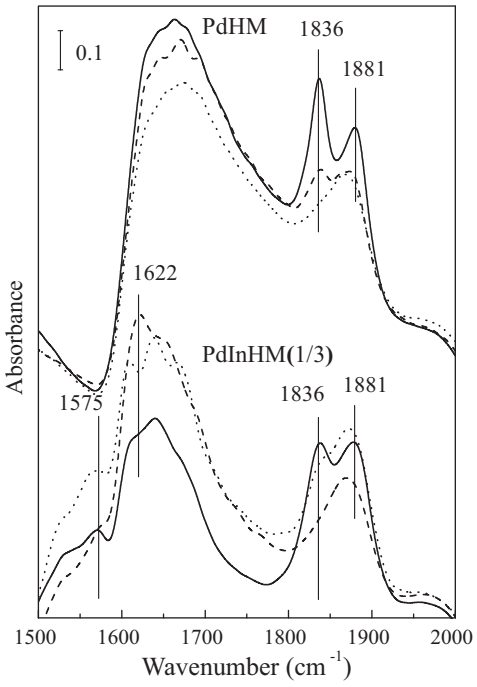

Fig. 9. FTIR spectra of adsorbed NO on calcined PdInHM(1/3) and calcined PdHM. Solid lines: spectra to 25 °C; dash lines: spectra to 100 °C; dot lines: spectra to 200 °C.

4. Conclusions

The effect of the addition of Pd to InHM catalysts depends on the In loading of the sample. For low In loading, PdInHM(1/6), the presence of 0.5 wt% of Pd results in a small decrease in the catalyitic activity for the NO_x to N_2 conversion. For higher In loading, PdInHM(1/3), the addition of Pd results in an increase in the catalytic activity which is more pronounced after certain time-on-stream at 500 °C.

CO adsorption experiments followed by FTIR measurements indicate the presence of Pd^+ and Pd^{2+} species, and that some formation of Pd^0 evolved with the CO exposure and/or after reduction with hydrogen. The TPR experiments indicate that the majority of In is under the form of $(InO)^+$ active sites. The Pd–In interactions in the bimetallic samples are interpreted in terms of the mobility of Pd, giving place to its migration towards sites of low accessibility in the case of the PdInHM(1/6) sample, and to the occurrence of Pd–In entities which are readily available to the reaction medium in the case of the PdInHM(1/3) sample. Another important effect originated by the different Pd/In ratio is observed in N_2 adsorption experiments in which PdInHM(1/3) and InHM(1/3) have a lower surface area than the corresponding PdInHM(1/6) and InHM(1/6) catalysts. These characteristics of the samples modify the interactions with NO_x molecules during the reaction. NO adsorption followed by FTIR shows more intense signals for the 1/3 bimetallic catalyst. These signals correspond to nitrate/nitrite species related to the presence of Pd^{+2} cations and NO_2 adsorbed on $(InO)^+$ sites. The balance between these species gives place to a maximum NO_2/NO ratio observed in the NO-TPD experiments for PdInHM(1/3), which correlates with the high activity of this sample.

Acknowledgements

The authors wish to thank UNL, CONICET and ANPCyT for their financial support and the Japan International Cooperation Agency for the donation of most of the instruments used in the development of this work. Thanks are given to Elsa Grimaldi for the English language editing and to Claudio Maitre for the technical assistance. One of the authors (J.V.) wish to thank for the financial support of the Hungarian Research Found (OTKA no. K-69052). Thanks are also due to the Hungarian-Argentinean program (HU/PA05-EXIV/002) that made this joint project possible.

References

[1] Y. Sato, H. Yu-u, N. Mizuno, M. Iwamoto, Appl. Catal. 70 (1991) L1–L5.
[2] H. Hamada, Y. Kintaichi, M. Sasaki, T. Ito, M. Tabata, Appl. Catal. 64 (1990) L1–L4.
[3] M. Iwamoto, H. Hamada, Catal. Today 10 (1991) 57–71.
[4] Y. Nishizaka, M. Misono, Chem. Lett. (1993) 1295.
[5] B.J. Adelman, W.M.H. Sachtler, Appl. Catal. B 14 (1997) 1–11.
[6] L.J. Lobree, A.W. Aylor, J.A. Reimer, H.V. Bell, 2nd World Congress on Environmental Catalysis, Miami, 1998 (Abstract 1–3).
[7] Y. Li, J.N. Armor, J. Catal. 145 (1994) 1–9.
[8] Y. Li, J.N. Armor, Appl. Catal. B 1 (1992) L31–L40.
[9] Y. Li, J.N. Armor, Appl. Catal. B 3 (1993) L1–L11.
[10] K. Yogo, S. Tanaka, M. Ihara, T. Hishiki, E. Kikuchi, Chem. Lett. (1992) 1025.
[11] K. Yogo, M. Ihara, I. Terasaki, E. Kikuchi, Appl. Catal. B Environ. 2 (1993) L1–L5.
[12] E. Kikuchi, K. Yogo, Catal. Today 22 (1994) 73–86.
[13] E. Kikuchi, M. Ogura, Catal. Surv. Jpn. 1 (1997) 227.
[14] M. Ogura, M. Hayashi, E. Kikuchi, Catal. Today 45 (1998) 139–145.
[15] M. Ogura, Y. Sugiura, M. Hayashi, E. Kikuchi, Catal. Lett. 42 (1996) 185.
[16] T. Sowade, C. Scmidt, F.W. Schutze, H. Berndt, W. Grunert, J. Catal. 214 (1) (2003) 100–112.
[17] J.A.Z. Pieterse, E.W. Van den Brink, S. Booneveld, F.A. Bruijn, Appl. Catal. B 46 (2003) 239–250.
[18] E. Kikuchi, M. Ogura, N. Aratani, Y. Sugiura, S. Hiromoto, K. Yogo, Catal. Today 27 (1996) 35–40.
[19] T. Sowade, T. Liese, C. Schmidt, F.-W. Schütze, X. Yu, H. Berndt, W. Grünert, J. Catal. 225 (2004) 105–115.
[20] Laura Gutierrez, Laura Cornaglia, E. Miró, J. Petunchi, Stud. Surf. Sci. Catal. 130 (2000) 1535–1540.
[21] Ferenc Lónyi, Solt Hanna E., József Valyon, Hernán Decolatti, Laura B. Gutierrez, Eduardo Miró, Appl. Catal. B Environ. 100 (2010) 133–142.
[22] T.C. Chang, J.J. Chen, C.T. Yeh, J. Catal. 96 (1985) 51–57.
[23] X. Zhou, Z. Xu, T. Zhang, L. Lin, J. Mol. Catal. A: Chem. 122 (1997) 125–129.
[24] M.A. Ulla, L. Gutierrez, E.A. Lombardo, F. Lónyi, J. Valyon, Appl. Catal. A. Gen. 277 (2004) 227–237.
[25] M. Armandi, B. Bonelli, E. Garrone, M. Ardizzi, F. Cavani, L. Dal Pozzo, L. Maselli, R. Mezzogori, G. Calestani, Appl. Catal. B: Environ. 70 (2007) 585–596.
[26] V. Gruver, J.J. Fripiat, J. Phys. Chem. 98 (1994) 8549–8554.
[27] K.I. Hadjiivanov, G.N. Vayssilov, Characterization of oxide surfaces and zeolites by carbon monoxide as an IR probe molecule, Adv. Catal. 47 (2002) 307, and references therein.
[28] A. Aylor, L. Lobree, J. Reimer, A.T. Bell, J. Catal. 172 (1997) 453–562.
[29] Konstantin I. Hadjiivanov, Georgi N. Vayssilov, Adv. Catal. 47 (2002) 307–511.
[30] K. Chakarova, E. Ivanova, K. Hasjiivanov, D. Klissurski, H. Knözinger, Phys. Chem. Chem. Phys. 6 (2004) 3702.
[31] C. Descorme, P. Gélin, M. Primet, C. Lécuyer, Catal. Lett. 41 (1996) 133–138.
[32] C. Descorme, P. Gélin, C. Lécuyer, M. Primet, J. Catal. 133 (1998) 352–362.
[33] Ken-ichi-Shimizu, Fumio Okada, Yasuhisa Nakamura, Atsushi Satsuma, Tadashi Hattori, J. Catal. 195 (2000) 151–160.
[34] A.R. Beltramone, L.B. Pierella, F.G. Requejo, O.A. Anunziata, Catal. Lett. 91 (1–2) (2003) 19–24.